Chinese Journal of Physiology 54(6): 427-434, 2011
DOI: 10.4077/CJP.2011.AMM114

Vulnerability in Simulated Ischemic Ventricular Transmural Tissues

Hong Zhang[1], Juan Wang[1], Lin Yang[2], Rui-juan Wu[1], Xi Mei[3], and Wei Zhao[1]

[1]*State Key Laboratory of Power Equipment and Electrical Insulation, School of Electrical Engineering, Xi'an Jiaotong University, Xi'an 710049*
[2]*Cardiology Department, the First Hospital, Xi'an Jiaotong University, Xi'an 710061*
and
[3]*Key Laboratory of Biomedical Information Engineering of Education Ministry, School of Life Science and Technology, Xi'an Jiaotong University, Xi'an 710049*
Shaanxi, People's Republic of China

Abstract

Vulnerability is an effective index to evaluate increased risk for unidirectional conduction block and reentry in hearts. Recent reports in animal experiments have indicated an opposite characteristics of the vulnerability in normal and ischemic transmural tissues. In order to clarify the differences and to investigate the mechanisms, a computer simulation method was used in this study to investigate the vulnerability relative to the premature pacing sites in normal and ischemic transmural tissues. Endo-, mid- and epi-cardial myocytes incorporating different severities of ischemia were developed across a tissue strand. The sodium channel inactivation gating variable *h* was calculated to provide the degree of sodium current recovery preceding the premature pacing. In the normal tissue, the measured vulnerable window was demonstrated to be wider by delivering an endocardial premature beat than that by applying an epicardial premature pacing. On the contrary, during ischemia the epicardium showed a wider vulnerable window than the endocardium. The results illustrated that during ischemia *h* decreased with accumulation of $[K^+]_o$, and action potential duration dispersion was obviously altered due to anoxia. In contrast, the elevated $[K^+]_o$ was suggested to play an important role in the difference of the location-dependent vulnerability in normal and ischemic tissues.

Key Words: arrhythmia, computer simulation, excitability, ischemia, vulnerable window

Introduction

It is an important medical issue to understand the reasons why and in what conditions ventricular tachycardias and fibrillations (VTs/VFs) occur since such arrhythmias are life threatening. There is a growing body of evidence to suggest that reentry, which is associated with spatial dispersions of repolarization and dynamic factors, plays a significant role in VTs/VFs (11, 12).

Recently, we used the ventricular wedge preparations to investigate the effects of stimulation sequence and location on the vulnerability to reentry. The results demonstrated that compared with premature beats at the epicardium, the vulnerable window induced by an extrasystole at the endocardium was wider (4), implying that the premature pacing at the endocardium was more likely to induce ventricular arrhythmias. The result was in good agreement with another report (19). However, a study in canine ischemic preparations suggested that the epicardial extrasystole was easier to induce reentry (24). This finding seems contrary to the results observed in normal perfused tissues.

Ischemia has been proved to easily induce reentry and even degenerated VF (3, 11); however, how the transmural dispersion in repolarization changes during acute global ischemia and its relationship to reentry

Corresponding author: Hong Zhang, Ph.D., School of Electrical Engineering, Xi'an Jiaotong University, 28 West Xianning Road, Xi'an 710049, Shaanxi, People's Republic of China. Tel: +0086-29-82668630-104, E-mail: maxr@263.net
Received: November 23, 2010; Revised (Final Version): June 2, 2011; Accepted: June 8, 2011.
©2011 by The Chinese Physiological Society and Airiti Press Inc. ISSN : 0304-4920. http://www.cps.org.tw

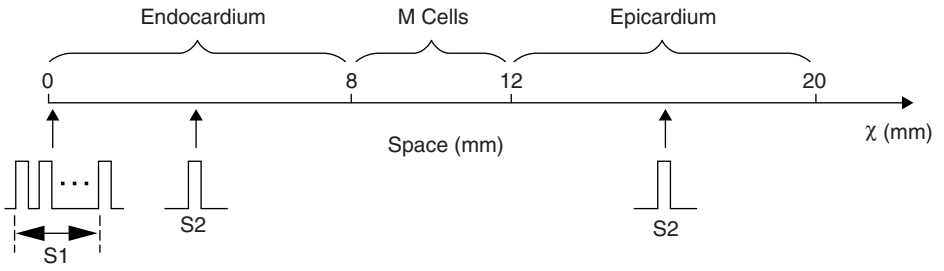

Fig. 1. Schematic diagram of the developed tissue strand and pacing protocols. The whole length of the strand was 20 mm in which the left-hand segment from 0-8 mm was the endocardium, the right-hand segment from 12-20 mm was the epicardium while the middle part between them was the midmyocardium. Basic stimuli S1 were delivered at the distal left-hand end of the endocardium. The premature pacing S2 was applied at the central segment of either the endocardium or the epicardium.

initiation and maintenance are only partially known today. To clarify the different results about the vulnerability between normal and ischemic tissues, we used in this work a computational approach to investigate effects and mechanisms of vulnerability in relation to the pacing sites.

Materials and Methods

Development of the Transmural Tissue Strand

The guinea pig ventricular cell models specified by Noble *et al*. (15, 16) were used to develop a one-dimensional tissue strand which can be described by the reaction-diffusion equation in [I] and the impermeable boundary conditions in [II] below:

$$\frac{\partial V}{\partial t} = -f(V, u)C_m^{-1} + D\frac{\partial^2 V}{\partial^2 x} \qquad [I]$$

$$\left.\frac{\partial V}{\partial x}\right|_{x = x_{\min}, x_{\max}} = 0 \qquad [II]$$

where V is the transmembrane potential, C_m is the membrane capacitance, u is a vector of the activation and inactivation gating variables and the ionic concentrations that determine the total membrane current $f(V, u)$, D is the diffusion coefficient for V, x is the spatial coordinate, and $x_{\min}$ and $x_{\max}$ represent the left- and right-hand ends of the strand, respectively. In the study, the strand consisted of 200 cells that were electrically coupled with two immediate neighbors by gap junctions, therefore, $x_{\min} = 0$ and $x_{\max} = 199$. The whole length of the strand was 20 mm due to the spatial step of 0.1 mm. $D = 23.25$ mm^2/s and $C_m = 0.0002$ μF were chosen for the simulation. A time splitting method was used to integrate the model as explained in Zhang *et al*. (26).

Previous studies have found heterogeneity of action potential duration (APD) across the mammal ventricular wall (6). Different densities of the rapid (I_{Kr}) and slow (I_{Ks}) delayed rectifier potassium currents are reported to be responsible for the heterogeneity. Therefore, by altering the ratios of the maximum conductance of I_{Kr} and I_{Ks}, a heterogeneous density distribution was introduced. According to previous reports (1, 22), the ratios were set to be 23:1, 15:1 and 7:1 for the epi-, endo- and mid-myocytes, respectively. Other differences such as the presence of a large I_{to} in the epicardium in certain species that could affect morphology of the action potential were not considered. As shown in Fig. 1, along the tissue strand, the proximal left-hand 8-mm segment was set to be the endocardium, the right-hand 8-mm segment simulated the epicardium, while the segment between them was the mid-myocardium.

Ischemia is a common cause of arrhythmias which can lead to very complicated physiological changes (2). To address the issue more realistically, three major component conditions of acute ischemia that affect electrophysiology were introduced: [1] the accumulation of extracellular K^+ concentration $[K^+]_o$, [2] intracellular and extracellular acidosis (decrease in pH), and [3] anoxia and metabolic blockade. The effects of acidosis were simulated through a decrease of G_{Na} and G_{CaL} in the Na^+ and Ca^{2+} channels, and a slight decline of the intracellular K^+ concentration $[K^+]_i$. Anoxia was approximated by reducing the intracellular ATP concentration $[ATP]_i$ which affects the ATP-dependent K^+ channels.

Observations have suggested that despite a greater susceptibility of the endocardium to metabolic effects of ischemia, electrophysiological changes that were evoked by ischemia in the epicardium were actually greater (17). Further demonstration have indicated that during ATP depletion, the shortening in APD was significantly greater in the epicardium than in the endocardium because of the much more evoked currents through ATP-dependent K^+ channels in the epicardium (5, 13, 18). Therefore, to simulate different electrophysiological changes to ischemia on

Table 1. Parameters of the three types of ischemic myocytes

	$[K^+]_o$	Anoxia	Acidosis		
	$[K^+]_o$ (mM)	ATP_i (mM)	G_{Na} (μS)	G_{CaL} (nA/mM)	$[K^+]_i$ (mM)
Endocardium	6.0	6.5	2.2	0.20	142.0
Midmyocardium	8.0	5.0	1.9	0.18	137.0
Epicardium	10.0	3.5	1.6	0.16	132.0

the normal transmural strand, five parameters of $[K^+]_o$, G_{Na}, G_{CaL}, $[K^+]_i$ and $[ATP]_i$ were set differently for the three types of myocytes as shown in Table 1 in which $[K^+]_i$ were the initial values of the dynamic $[K^+]_i$. It was reported that at about 10 min of ischemia, $[K^+]_o$ was approximately 12 mM, the acidic pH was about 6.5 and anoxia reduced ATP_i to 3.0 mM (2, 21). According to the reported experimental observations (7-9) in Ref. 21, sodium conductance, calcium conductance and $[K^+]_i$ were reduced about 25%, 25% and 10%, respectively, to simulate the state of pH = 6.5. Hence, we selected each value at about the same time less than 10 min for epicardial myocytes. Based on that, the heterogeneity of ischemia along the fiber was considered.

Vulnerable Window and Recovery of Excitability

Vulnerable window (VW) defines a temporal window within which a unidirectional conduction block or reentrant excitation can be induced. The wider the VW, the higher the probability is for the reentrant initiation (4). The time VW was determined by an extra-stimulus technique in this study. Fig. 1 shows the pacing protocols used in the measurement of the vulnerability. In reality, the activation sequence during the sinus rhythm typically proceeds from the endocardium to the epicardium, therefore, in experiments basic stimuli S1 were exerted at the distal left-hand end of the endocardium. Then, a premature pacing S2 was applied at the center of either the endocardium or the epicardium. The S1 S2 coupling interval progressively increased with 1 ms increment. VW was defined as the period between the onset of unidirectional block and the onset of bidirectional conduction. As calculated by Shaw and Rudy (20), VW was the time difference between the occurrence of the last bidirectional block and the occurrence of the first bidirectional conduction.

Recovery of the cellular excitability is determined by the voltage-dependent kinetics of sodium channel recovery. The inactivation gating variable *h* in the model can provide the degree of sodium current recovery and the fraction of available sodium channels. Therefore, *h* was used to reflect the degree of excitability.

In the experiments, three component conditions of acute ischemia were applied individually and in combination for the measurement of VW and the identification of ionic mechanisms. All stimulations during the experiments were 2 ms in duration and twice-diastolic threshold current (30 μA/μF).

Results

Normal Conditions

Fig. 2 displays action potentials (A) and their corresponding *h* (B) produced by the endocardial pacing S1 in the developed normal transmural tissue strand, and three computed space-time plots of response to a premature pacing S2 (C to E). The resting tissue was activated at the endocardial end by eight consecutive basic stimuli S1 with the coupling interval of 800 ms. The delivery time of the latest S1 was set at $t = 0$, then a pacing S2 was applied at a time $t = T$ during late repolarisation. As T was varied, there were three types of behavior. As noted in Fig. 2C, S1 induced activation propagated from the endocardium to the epicardium, causing a time delay upon the upstroke of action potentials at different sites. Three types of myocytes located in the middle of each layer displayed different APDs in Fig. 2A. Endo-, mid- and epi- myocytes had APDs of 197 ms (bold line), 224 ms (broken line) and 184 ms (thin line), respectively, demonstrating a longest APD in mid-myocytes. Thus, in Fig. 2C the middle segment of the strand repolarized later than the epicardium although the mid-myocytes activated earlier. Moreover, the conduction velocity of 274 mm/s was found to be consistent along the strand without showing the impact from different APDs. Due to the homogenizing effects of cell-to-cell coupling presented in the tissue, the smooth transitions between different types of layers could also be observed in Fig. 2C.

Fig. 2B shows *h* corresponding to action potentials in Fig. 2A. Each *h* was 99% recovered after 35 ms of the preceding repolarization (differences secondary to APD difference should not be considered).

Fig. 2C to Fig. 2E display three behaviors after S2 was applied at the endocardium. At T = 200 ms

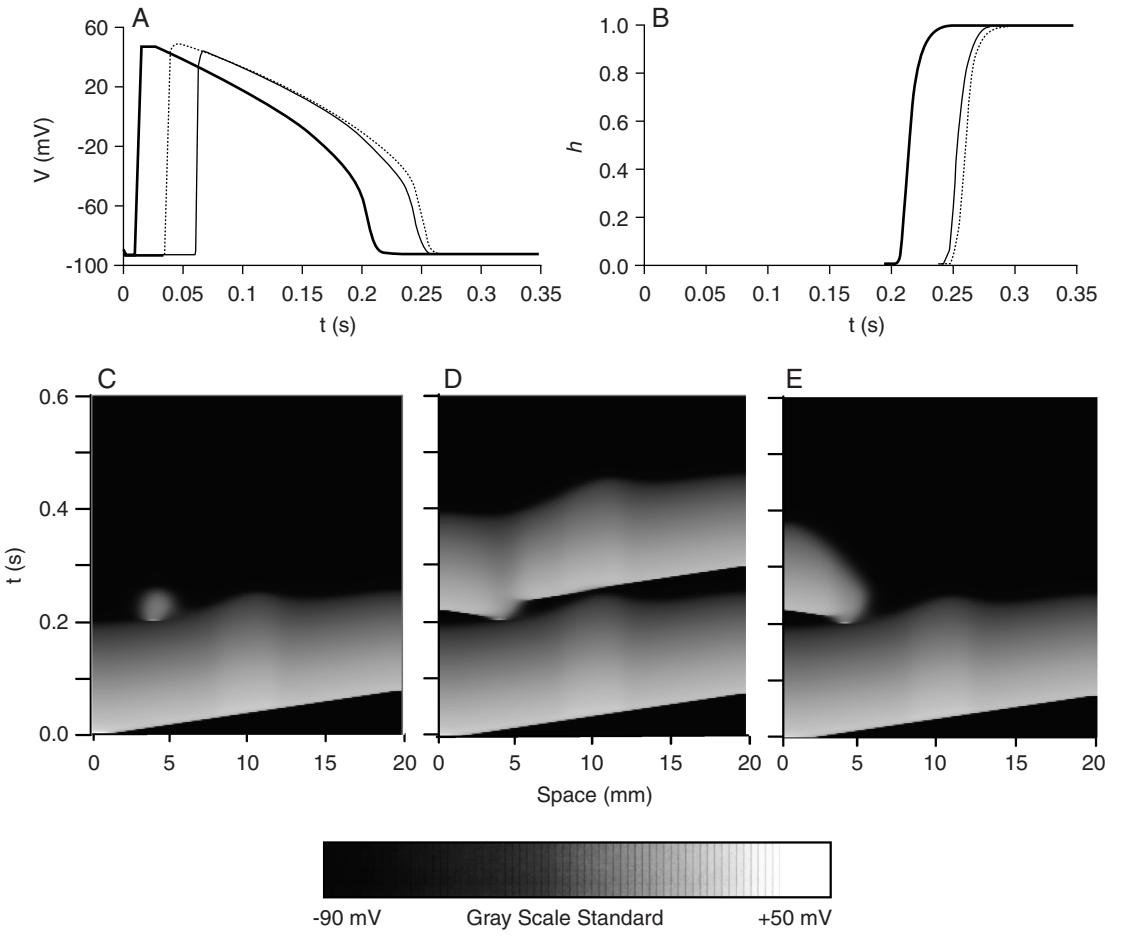

Fig. 2. Electrical activities in the developed normal transmural tissue strand. A and B: action potentials and their corresponding *h* for the endo- (bold line), mid- (broken line) and epi- (thin line) myocytes located at the sites of 4, 10 and 16 mm, respectively. C to E: three computed space-time plots of the membrane potential response to an endocardial premature pacing S2. C: bidirectional conduction block. D: bidirectional propagation. E: unidirectional propagation.

after the delivery time of the latest S1 (Fig. 2C), cells on either side of the strand were still in the refractory period of the preceding action potential, resulting in the last bidirectional block. A small local electrotonus caused by S2 could not induce an excitable wave, thus, a failure of electrical propagation. At T = 205 ms, cells on both sides had fully recovered from the preceding activation, producing the first bidirectional conduction (Fig. 2D). At T = 203 ms (Fig. 2E), cells on the right-hand side could not be activated thereby initiating a unidirectional propagation. Therefore, the measured VW was 5 ms for the endocardial pacing S2. If S2 was delivered at the epicardium, a VW of less than 1 ms was observed, illustrating a greater endocardial vulnerability in the normal tissue.

Anoxia

Anoxia was simulated by lowering $[ATP]_i$ and activating the ATP-sensitive K^+ current. The effects of anoxia on action potentials (A), *h* (B) and vulnerability (C to E) of the developed stand are shown in Fig. 3. In Fig. 3A, for the middle sited endo-, mid- and epi-myocytes, APD became 185 ms (bold line), 172 ms (broken line) and 128 ms (thin line), respectively. Each *h* was 99% recovered after 35 ms of the preceding repolarization (Fig. 3B). For an epicardial premature pacing S2, T = 175 ms corresponded to the last bidirectional conduction block (Fig. 3C), T = 180 ms led to the first bidirectional propagation (Fig. 3D) while T = 177 ms caused a unidirectional propagation (Fig. 3E). Therefore, VW was 5 ms. For the endocardially delivered pacing S2, the measured VW was 4 ms.

Increased $[K^+]_o$

As shown in Fig. 4, the increase of extracellular potassium caused elevation of the resting potential and shortening of APD as well. For the endo-, mid-

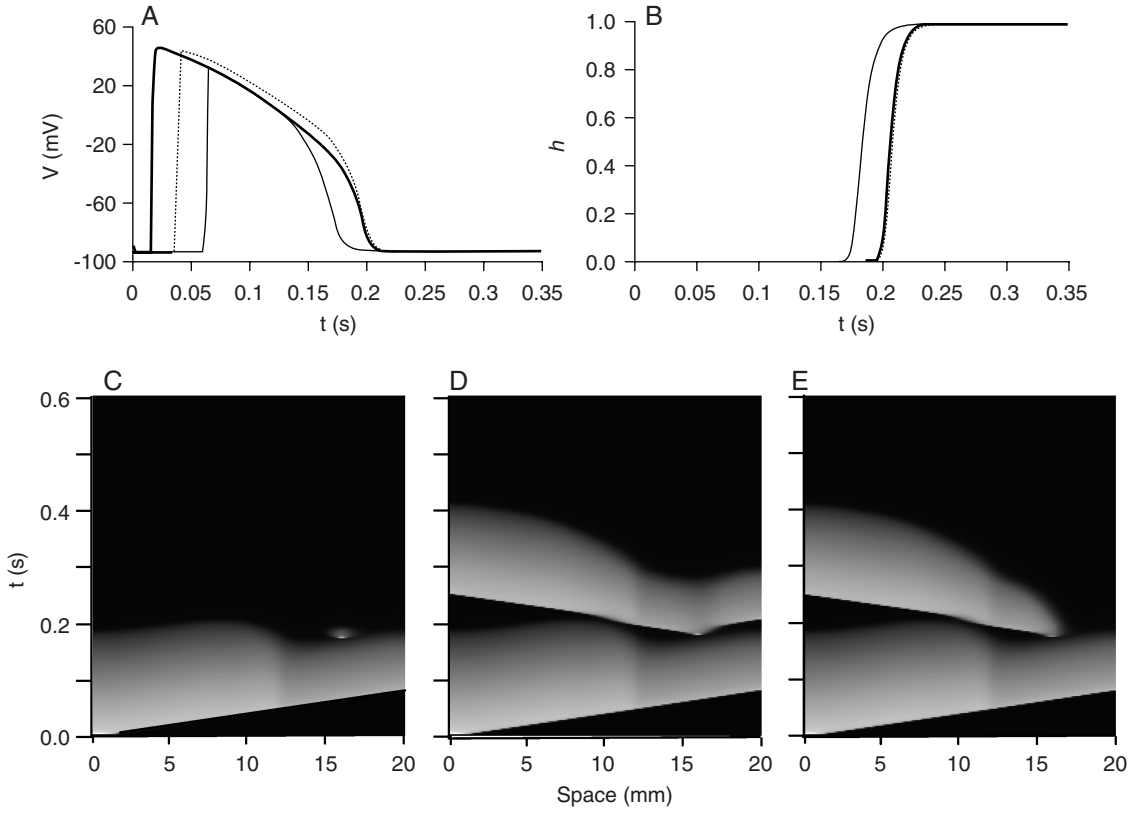

Fig. 3. Effects of anoxia on action potentials (A) and their corresponding *h* (B) for the endo- (bold line), mid- (broken line) and epi- (thin line) myocytes. C to E: representative space-time plots of the membrane potential at an epicardial premature pacing S2.

and epi-myocytes, APDs became 179 ms, 177 ms and 152 ms, respectively (Fig. 4A). Differently elevated $[K^+]_o$ caused a different recovery time and fraction of *h*: the endocardium recovered 95% after 101 ms, the midmyocardium needed 80 ms to recover 70%, and the epicardium recovered only 53% after 150 ms. The results demonstrated that *h* became small and needed a long recovery time with the increase of $[K^+]_o$. In addition, for an epicardial pacing S2, the last blocked (Fig. 4C) and the first bidirectional (Fig.4D) propagations occurred at T = 212 ms and 221 ms, respectively, resulting in a VW of 9 ms. But for the endocardial pacing S2, the measured width of VW was only 2 ms.

Acidosis and the Three Combined Conditions

During acidosis, the decrease of G_{Na} , G_{CaL} and $[K^+]_i$ caused about 1.3 mV depolarization of resting membrane potential and a slight APD shortening (Fig. 5A). For each type of myocytes, APD became 192 ms (endocardium), 217 ms (midmyocardium) and 179 ms (epicardium). The recovery of excitability was almost unchanged (Fig. 5B) in contrast with the normal conditions. The measured VW corresponded to 2 ms and 5 ms for an epicardial and endocardial pacing S2, respectively. Therefore, compared with the effects of anoxia and $[K^+]_o$ accumulation, the electrophysiological effects of acidosis were insignificant.

Figs. 5C and 5D show the action potentials and *h* in combination of the three acute ischemic components. In the middle of each layer, APD became 170 ms for the endocardium (bold line), 133 ms for the midmyocardium (broken line) and 101 ms for the epicardium (thin line). APDs of the epicardium were greatly reduced because of the most severe ischemia. The average conduction velocity across the transmural wall decreased to 232 mm/s. When S2 was delivered at the epicardium, the measured VW was 11 ms which was larger than 5 ms measured through the endocardial premature pacing.

Discussion

In this study, we used a simulation method to investigate the vulnerability in relation to the location of the premature pacing. Three types of myocyte were developed along a normal tissue strand in which mid-myocytes exhibited the longest APDs while the epicardium showed the shortest ones (Fig. 2A). Based on the reports that ischemia-induced electrophysiological changes were greater in the epicardium than in

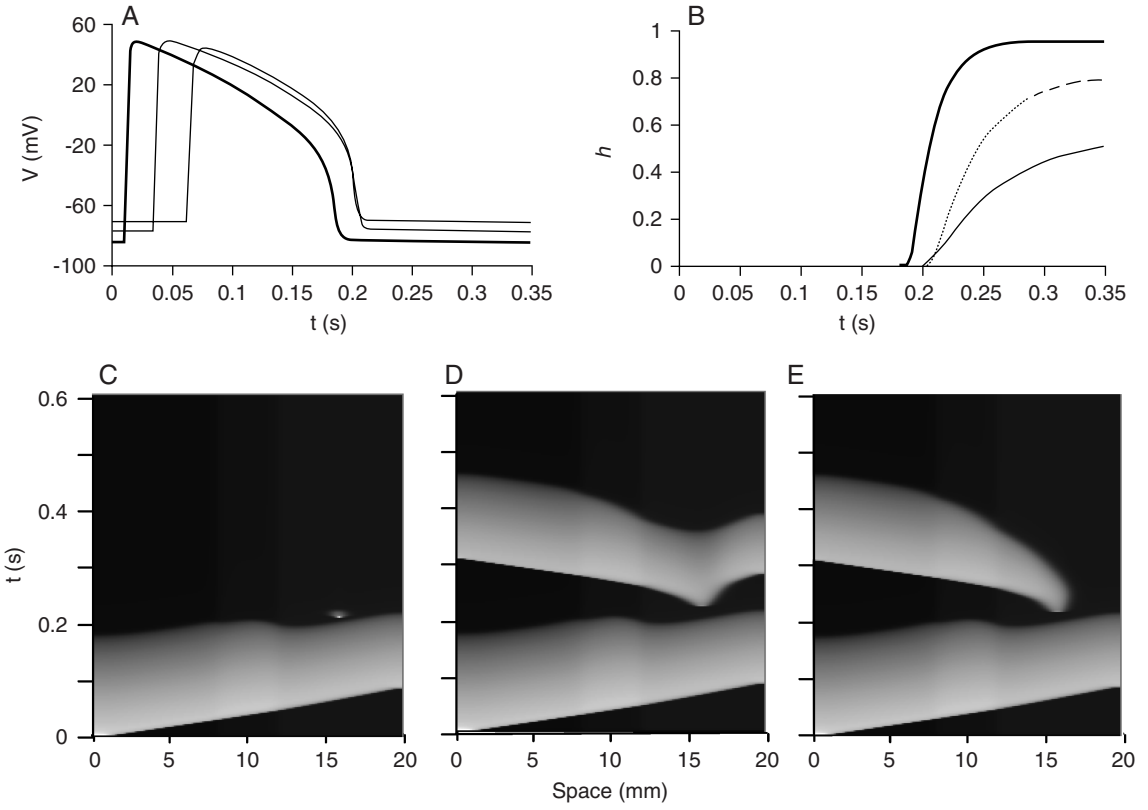

Fig. 4. Effects of $[K^+]_o$ accumulation on action potentials (A) and their corresponding *h* (B) for the endo- (bold line), mid- (broken line) and epi- (thin line) myocytes. C to E: three space-time plots of the membrane potential at an epicardial premature pacing S2.

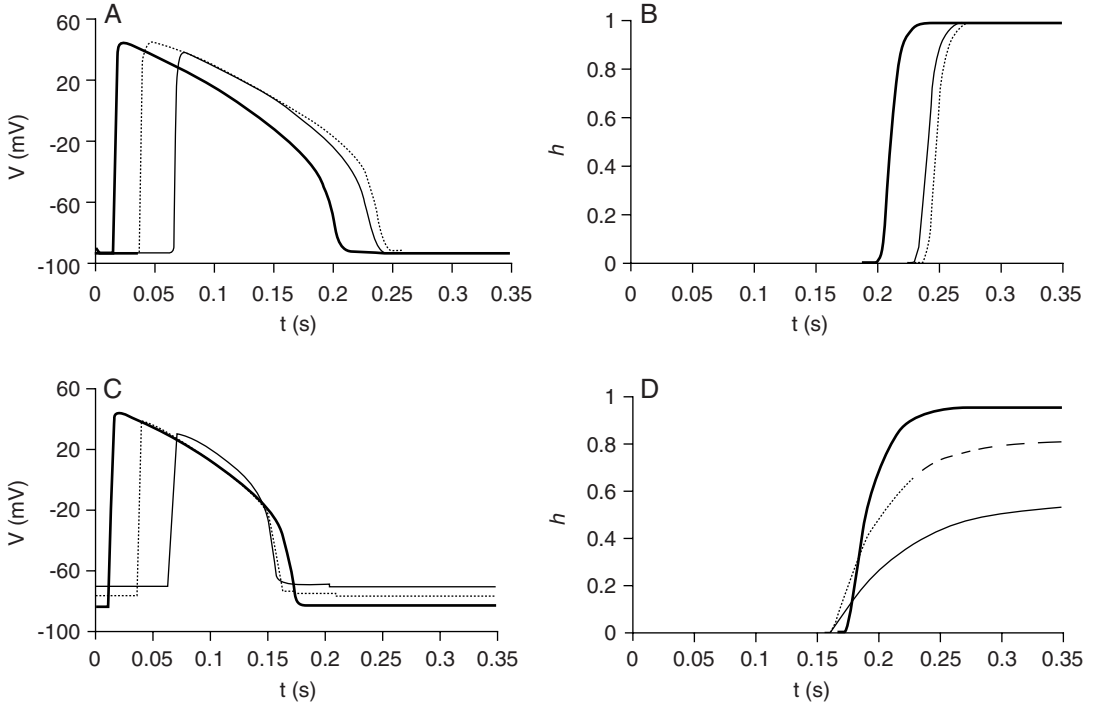

Fig. 5. Action potentials and *h* corresponding to acidosis (A and B) and three combined ischemic components of anoxia, $[K^+]_o$ accumulation and acidosis (C and D).

the endocardium (17, 18), five parameters responsible for the major electrophysiological alterations in action potential morphology and propagation were altered differently for three types of myocytes to take different severities of ischemia into consideration.

The ischemic myocytes showed typical characteristics: elevated resting potential, shortened APDs and declined amplitudes of action potentials (Fig. 5C). The more severe the ischemia was, the more remarkable these properties were. The observations were in good agreements with other studies (3, 25, 26). Compared with normal conditions (Fig. 2A), for the epicardial myocytes the shortened APDs due to anoxia (Fig. 3A), $[K^+]_o$ accumulation (Fig. 4A) and acidosis (Fig. 5A) were about 30%, 17% and 2%, respectively. The elevation of $[K^+]_o$ caused 25% depolarization of the resting potential and 46% reduction of h while anoxia and acidosis had very minor impact. Therefore, anoxia-dependent activation of $I_{K(ATP)}$ was suggested to be a major factor of the APD shortening in ischemia. But the depression and delayed recovery of membrane excitability was mainly caused by the elevation of $[K^+]_o$.

Under normal conditions (Fig. 2), the width of VW at an endocardial pacing S2 was demonstrated to be wider than that at an epicardial premature pacing. The result was in agreement with our previous experimental study (4) and the report (19) in which a single endocardial extrasystole arising from the endocardium was demonstrated to need much lower critical gradient in refractoriness than a single extrasystole originating from the epicardium, implying that a premature pacing in the endocardium was easier to elicit a unidirectional propagation.

However, during ischemia, as measured in Fig. 3, anoxia increased the epicardial width of VW, making VW become slightly larger than at an endocardial pacing S2. Accumulation of $[K^+]_o$ could also cause an increase of the epicardial VW (Fig. 4), resulting in an obviously greater VW than that originating from the endocardial premature pacing. But acidosis alone showed minor effects on vulnerability. Anoxia was the main cause of APD shortening during ischemia. In contrast with the normal conditions in which mid-myocytes showed the longest APD (Fig. 2), during anoxia (Fig. 3), from the endocardium to the epicardium, the altered APD formed a new APD dispersion which caused the location-dependent vulnerability. However, in contrast (Figs. 3 and 4), accumulation of $[K^+]_o$ had much greater impacts on VW than anoxia. Accumulation of $[K^+]_o$ not only caused APD shortening as reported (14, 23), it also led to depolarization of the resting potential and, thus, the change of cellular excitability. During accumulation of $[K^+]_o$, h could not reach 100% after the preceding action potential (Fig. 4B) indicating a decreased fraction of available sodium channels and a small degree of sodium current recovery for the following production of action potentials. Thus, the elevated $[K^+]_o$ delayed myocytes to recover excitability beyond the return to the resting potential leading to a post-repolarization refractoriness. With the severity of ischemia, the excitability was depressed further, and the post-repolarization refractoriness became much longer. As noted in Fig. 4, compared with the higher excitability of the mid- and endo-myocytes that facilitated the critically timed activation induced in the epicardium to propagate among them, the lower excitability of the epicardium prevented the activation wave from spreading to the right side, thereby causing a decremental or failed electrical conduction in the epicardium. On the other hand, the transmural dispersion of excitability facilitated the extrasystole elicited at the endocardium to propagate along two directions of the strand though with a gradually decreased velocity, resulting in a low probability of the unidirectional block. Therefore, the epicardial VW was wider than that measured at the endocardium.

Cellular excitability and APD dispersion both seemed to play important roles in determining the vulnerability. During normal conditions, without heterogeneity of the excitability across the transmural wall, APD dispersion became a predominate factor in determining the wider endocardial VW. During ischemia, the transmural gradient of excitability and the change of APD dispersion arising from accumulation of $[K^+]_o$ and anoxia formed the substrate for the wider epicardial VW. However, in contrast, the elevated $[K^+]_o$ was shown to bear the main responsibility. Although $[K^+]_o$ accumulation could also shorten APD, compared with anoxia, APD shortening by $[K^+]_o$ accumulation was much less than during anoxia, indicating a more important role of excitability in the location-dependent VW during ischemia.

In this study, a transmural strand with different severities of ischemia was developed to study mechanisms of the location-dependent vulnerability in the normal and ischemic tissue. Although the transmural model could simulate main characteristics of the three types of myocytes, it was simple without considering other differences such as I_{to} shown in certain species. Additionally, since the model equations have no relevant ion channels related directly to pH values, we reduced the initial value of $[K^+]_i$ to simulate an effect of acidosis. As reported previously (10), with low initial value of $[K^+]_i$, the steady state concentration of $[K^+]_i$ was also kept low, but with the same value for the different sets of initial conditions. Therefore, in the simulations the different low $[K^+]_i$ effects in acidosis were only valid in the initial stage. Because $[K^+]_i$ showed very little impact in the study, the limit would have minor effects on the conclusions.

It is known that the vulnerable window is an effective index to evaluate the increased risk for reentry; therefore, the results in this study indicated that during ischemia the clinical VT induction by a premature ventricular complex was easier in the epicardium than that in the endocardium. In this case, the ischemia-induced elevation of $[K^+]_o$ was suggested to be the main substrate for this kind of ventricular arrhythmia.

Acknowledgments

This study was supported by the National Natural Science Foundation of China (No. 30870659, 30971221), the Health Foundation of Shaanxi province in China (08D23), the Scientific Research Foundation for Returned Scholars, Ministry of Education of China (1028) and the Fundamental Research Funds for the Central Universities.

References

1. Akar, F.G. and Rosenbaum, D.S. Transmural electrophysiological heterogeneities underlying arrhythmogenesis in heart failure. *Circ. Res*. 93: 638-645, 2003.
2. Carmeliet, E. Cardiac ionic currents and acute ischemia: from channels to arrhythmias. *Physiol. Rev*. 79: 917-1017, 1999.
3. Cascio, W.E. Myocardial ischemia: What factors determine arrhythmogenesis? *J. Cardiovasc. Electrophysiol*. 12: 726-729, 2001.
4. Chen, X.Z., Zhang, H., Jin, Y.B. and Yang, L. Vulnerability to unidirectional conduction block and reentry in rabbit left ventricular wedge preparation: effect of stimulation sequence and location. *Chinese J. Physiol*. 52: 16-22, 2009.
5. Furukawa, T., Kimura, S., Furukawa, N., Bassett, A.L. and Myerburg, R.J. Role of cardiac ATP-regulated potassium channel in differential responses of endocardial and epicardial cells to ischemia. *Circ. Res*. 68: 1693-1702, 1991.
6. Henry, H. and Rappel, W.J. The role of M cells and the long QT syndrome in cardiac arrhythmias: simulation studies of reentrant excitations using a detailed electrophysiological model. *Chaos* 14: 172-182, 2004.
7. Irisawa, H. and Sato, R. Intra- and extracellular actions of proton on the calcium current of isolated guinea pig ventricular cells. *Circ. Res*. 59: 348-355, 1986.
8. Kagiyama, Y., Hill, J.L. and Gettes, L.S. Interaction of acidosis and increased extracellular potassium on action potential characteristics and conduction in guinea pig ventricular muscle. *Circ. Res*. 51: 614-623, 1982.
9. Kléber, A.G. Resting membrane potential, extracellular potassium activity, and intracellular sodium activity during acute global ischemia in isolated perfused guinea pig hearts. *Circ. Res*. 52: 442-450, 1983.
10. Livshitz, L. and Rudy, Y. Uniqueness and stability of action potential models during rest, pacing, and conduction using problem-solving environment. *Biophys. J*. 97: 1265-1276, 2009.
11. Lopshire, J.C. and Zipes, D.P. Sudden cardiac death: better understanding of risks, mechanisms, and treatment. *Circulation* 114: 1134-1136, 2006.
12. Michael, R. and Douglas, P.Z. Mechanisms of sudden cardiac death. *J. Clin. Invest*. 115: 2305-2315, 2005.
13. Michailova, A., Lorentz, W. and Mcculloch, A. Modeling transmural heterogeneity of KATP current in rabbit ventricular myocytes. *Am. J. Physiol. Cell Physiol*. 28: C542-C557, 2007.
14. Morena, H., Janse, M.J., Fiolet, J.W.T., Krieger, W.J.G., Crijns, H. and Durrer, D. Comparison of the effects of regional ischemia, hypoxia, hyperkalemia, and acidosis on intracellular and extracellular potential and metabolism in the isolated porcine heart. *Circ. Res*. 46: 634-646, 1980.
15. Noble, D., Noble, S.J., Bett, G.C., Earm, Y.E. and Ho, W.K. The role of sodium-calcium exchange during the cardiac action potential. *Ann. NY. Acad. Sci*. 639: 334-353, 1991.
16. Noble, D., Varghese, A., Kohl, P. and Noble, P. Improved guinea-pig ventricular cell model incorporating a diadic space, I_{kr} and I_{ks}, and length- and tension-dependent processes. *Can. J. Cardiol*. 14: 123-134, 1998.
17. Okumura, K., Horio, Y. and Matsuyama, K. Alterations in electrophysiological properties during canine myocardial ischemia: variation with location in the ischemic zone *in vivo*. *Jpn. Circ. J*. 47: 661-670, 1983.
18. Qi, X.Y., Shi, W.B., Wang, H.H., Zhang, Z.X. and Xu, Y.Q. A study on the electrophysiological heterogeneity of rabbit ventricular myocytes- the effect of ischemia on action potentials and potassium currents. *Acta Physiol. Sin.* 52: 360-364, 2000.
19. Qu, Z.L., Garfinkel, A. and Weiss, J.N. Vulnerable window for conduction block in a 1D cable of cardiac cells: 1. Single extrasystoles. *Biophysical J*. 91: 793-804, 2006.
20. Shaw, R.M. and Rudy, Y. The vulnerable window for unidirectional block in cardiac tissue: characterization and dependence on membrane excitability and intercellular coupling. *J. Cardiocvasc. Electrophysiol*. 6: 115-131, 1995.
21. Shaw, R.M. and Rudy, Y. Electrophysiologic effects of acute myocardial ischemia: a theoretical study of altered cell excitability and action potential duration. *Cardiocvasc. Res*. 35: 256-272, 1997.
22. Viswanathan, P.C., Shaw, R.M. and Rudy, Y. Effect of *Ikr* and *Iks* heterogeneity on action potential duration and its rate dependence. *Circulation* 99: 2466-2474, 1999.
23. Weidmann, S. The effect of the cardiac membrane potential on the rapid availability of the sodium-carrying system. *J. Physiol*. 127: 213-224, 1955.
24. Wu, J. and Zipes, D.P. Transmural reentry triggered by epicardial stimulation during acute ischemia in canine ventricular muscle. *Am. J. Physiol. Heart Circ. Physiol*. 283: H2004-H2011, 2002.
25. Yang, Z., Zhang, H. and Kong, S. Study for relevance of the acute myocardial ischemia to arrhythmia by optical mapping method. *Physiol. Meas*. 28: 481-488, 2007.
26. Zhang, H., Zhang, Z.X., Yang, L., Jin, Y.B. and Huang, Y.Z. Computer simulation study of the reentrant cardiac arrhythmias in ischemic myocardium. *Chinese J. Physiol*. 48: 155-159, 2005.